

Simultaneous Oxidation of Trace Organics and Sorption of Trace Metals by Ferrate (Fe(VI))-Coated Sand in Synthetic Wastewater Effluent

Published as part of ACS Environmental Au virtual special issue “2024 Rising Stars in Environmental Research”.

Fanny E. K. Okaikue-Woodi, Reyna Morales Lumagui, and Jessica R. Ray*



Cite This: ACS Environ. Au 2024, 4, 260–270



Read Online

ACCESS |

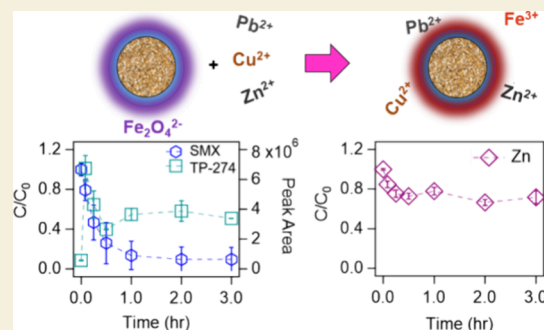
Metrics & More

Article Recommendations

Supporting Information

ABSTRACT: The increased presence of toxic chemicals in aquatic matrices and their associated health effects raise the need for more effective treatment technologies. The application of Fe(VI), an advanced oxidation treatment agent with disinfecting and coagulating capabilities, is limited by Fe(VI) aqueous instability. Our previous study proposed an Fe(VI)-coated sand media to overcome this constraint and demonstrated that Fe(VI)-coated sand was an effective medium for the treatment of phenolic compounds. In this study, we assessed the potential of the media for treatment of acetaminophen (ACM), benzotriazole (BZT), sulfamethoxazole (SMX), copper (Cu), lead (Pb), and zinc (Zn)—common contaminants found in wastewater effluents—in ultrapure and synthetic wastewater effluent. Fe(VI)-coated sand reactivity was influenced by the solution pH and aqueous chemistry. For example, the removal of Pb improved by 39% in the presence of trace organics, indicating that trace metal removal was enhanced by Fe(III) phases formed during Fe(VI) reactions with trace organics. While oxidation of trace organic compounds increased as pH decreased, trace metal sorption was more favorable at higher pH (i.e., pH 8 and 9). The oxidation efficiency of trace organics by the media was the highest for ACM and SMX while BZT degradation was limited due to formation of Cu–BZT complexes. Batch tests in synthetic wastewater effluent revealed that the presence of divalent cations (i.e., Ca^{2+} and Mg^{2+}) can catalyze Fe(VI) self-decay and promote Fe(III) production and subsequent trace metal removal; however, oxidation of trace organics was hindered in this matrix. This study highlights the potential for Fe(VI)-coated sand application for the treatment of complex matrices more representative of natural and engineered aquatic systems.

KEYWORDS: ferrate, oxidation, sorption, wastewater, composite



1. INTRODUCTION

Due to water shortages, wastewater effluent is increasingly considered for augmentation of water resources.¹ Treated wastewater discharges into nearby water bodies that often serve as downstream drinking water sources. Additionally, wastewater effluent can be injected into aquifers to recharge groundwater and replenish drinking water aquifers.¹ However, processes used in conventional wastewater treatment plants have variable effectiveness for the removal of trace contaminants prior to discharge.^{2,3} Studies have reported the presence of contaminants such as heavy metals^{4–6} and organic compounds (e.g., antibiotics,^{2,7} prescription drugs,^{2,8} and industrial chemicals³) in wastewater effluents. The increasing presence of these contaminants in wastewater effluent discharges and in reclaimed wastewater due to anthropogenic activity and overuse of chemicals may cause acute and chronic risks to human health and aquatic life^{8,9} and jeopardizes the safety of wastewater reuse and aquifer recharge efforts. For example, Ferrari et al. detected diclofenac, carbamazepine, and

clofibric acid in real wastewater effluent solutions and reported chronic effects when invertebrates obtained from laboratory cultures were exposed to the wastewater effluent solutions.¹⁰ Therefore, advanced treatment of wastewater effluents is necessary to decrease the trace contaminant load to receiving waters.

Many advanced (oxidation) treatment processes (e.g., ozonation, Fenton processes, UV irradiation, and reverse osmosis membrane filtration) have been proposed and investigated to enhance contaminant removal and degradation during wastewater treatment. Ferrate [Fe(VI)] is a multifunc-

Received: April 21, 2024

Revised: June 26, 2024

Accepted: June 27, 2024

Published: July 10, 2024



tional iron oxide capable of oxidation,^{11,12} coagulation,^{12,13} and disinfection^{14,15} with a standard oxidation potential (E^0) of 2.2 V, which is greater than the oxidation potential of chlorine (1.36 V),¹² a commonly used disinfectant and oxidant. For example, Yang et al. observed more than 90% removal of trace organic compounds by Fe(VI) in secondary wastewater effluent.¹⁶ Additionally, Fe(VI) is considered an environmentally benign chemical because it reduces into nontoxic Fe(III) species during application,^{11,17} which is often used as coagulants^{12,14} and adsorbents^{12,18} in water treatment. However, the use of Fe(VI) as a water treatment technology for contaminant destruction is limited due to its chemical instability in solution. As the solution pH increases to alkaline pH ranges (pH > 7.3), the Fe(VI) aqueous stability increases; however, its oxidizing power decreases.¹⁹ Previous studies have proposed methods to increase Fe(VI) oxidizing power at environmentally relevant pH and accelerate the oxidation of organic contaminants.^{20–25} For example, Manoli et al. observed a 47% increase in the oxidation of caffeine by Fe(VI) in the presence of SiO₂ gels.²⁵ SiO₂ reportedly promotes the formation of the more reactive Fe(V) and Fe(IV) intermediates²⁶ and retards the self-decomposition of Fe species.²⁵ In our previous work, we proposed and developed an Fe(VI)-coated sand composite media that leverages SiO₂ stabilization properties for enhanced water treatment applications.¹⁹ We observed 51% oxidation of phenol by the Fe(VI)-coated sand within 5 min of treatment compared to 37% when aqueous Fe(VI) powder was applied, which indicates enhanced oxidation efficacy by immobilizing Fe(VI) on the sand surface.¹⁹ Therefore, applying the Fe(VI)-coated sand media presents an opportunity for advancing water treatment processes with additional capabilities (i.e., oxidation, coagulation, and disinfection) due to the multimodal properties of Fe(VI). While our previous study indicated that the application of the Fe(VI)-coated sand media would be effective to degrade phenolic compounds in wastewater, there are many other types of chemical contaminants present in wastewater. Therefore, a better assessment of the Fe(VI)-coated sand performance should include more complex and varied matrices and contaminants.

In this study, we investigate the potential of Fe(VI)-coated sand media for advanced treatment of multiple contaminant classes and more environmentally representative aquatic matrices. Specifically, we evaluated the removal of trace metals (i.e., copper, lead, and zinc) and organic compounds (i.e., acetaminophen, sulfamethoxazole, and benzotriazole) commonly found in wastewater effluents. Copper (Cu), lead (Pb), and zinc (Zn) can enter wastewater from industrial sources (e.g., paper mills, textiles, paints, and oil refining)^{4,27} and household products (e.g., detergents).^{5,27} Acetaminophen (ACM) is a widely used nonprescription drug that has been widely detected in aquatic environments.^{2,28,29} Sulfamethoxazole (SMX) is an antimicrobial widely used in human and veterinary medicine^{30,31} and has been detected in wastewater effluents.^{30,32} Benzotriazole (BZT) is used as an anticorrosion agent and has also been detected in wastewater effluents.^{33,34} An advantage of Fe(VI) application is its reduction into Fe(III) species, thus enabling dual treatment of organic and inorganic contaminants by Fe(VI) in a single unit process. Therefore, the specific objectives of this study are to (1) assess the capacity of the Fe(VI)-coated sand for the treatment of a wider range of contaminants, (2) understand the competitive removal of organic and inorganic contaminants, and (3)

characterize the effects of the wastewater effluent matrix on the Fe(VI)-coated sand treatment rates.

2. MATERIALS AND METHODS

2.1. Chemicals

Acetaminophen (Spectrum Chemical MFG Corp, NJ), 1,2,3-benzotriazole (TCI America, OR), sulfamethoxazole (TCI America, OR), copper(II) chloride anhydrous (Thermo Fisher Scientific, WA), lead(II) chloride (Thermo Fisher Scientific, WA), zinc(II) chloride anhydrous (Thermo Fisher Scientific, WA), and sodium sulfite anhydrous (Na₂SO₃, Fisher Scientific, MA) were purchased to assess contaminant removal by the media. Details of all other chemicals used in this study can be found in Text S1 (in the Supporting Information). All experiments were conducted using ultrapure Milli-Q water (resistivity: 18.2 MΩ-cm).

2.2. Synthesis and Surface Characterization of Fe(VI)-Coated Sand

Fe(VI)-coated sand was synthesized as previously described in Okaikue-Woodi and Ray.¹⁹ Briefly, Ottawa sand, initially coated with tetraethylorthosilicate (TeOS), was added to a K₂FeO₄ solution and stirred for 24 h at 4 °C.¹⁹ The wet Fe(VI)-coated sand composite was dried under vacuum.¹⁹ Surface analyses of the media were conducted to complement aqueous in situ characterization analyses reported in our previous study.¹⁹ Scanning electron microscopy (SEM) imaging of the Fe(VI)-coated sand morphology was performed with a FEI (Hillsboro, OR) Sirion XL30 SEM instrument following platinum sputtering of the media to increase electrical conductivity. The elemental composition on the surface of the Fe(VI)-coated sand was also evaluated via SEM energy dispersive X-ray spectroscopy (SEM-EDS) following carbon coating of the media. X-ray diffraction measurements were recorded on a Bruker (Billerica, MA) D8 Discover X-ray diffractometer operated at 50 kV and 1000 μA. The scanning parameters were a 11° 2θ step size and 60 s/step over a 0–93° 2θ Cu Kα angular range.

2.3. Removal of Trace Metals and Organics in Ultrapure Water

Batch experiments were conducted to evaluate the Fe(VI)-coated sand removal capacity of the contaminants in a pure water matrix containing only 10 mM sodium borate buffer. Stock solutions of each contaminant were prepared in Milli-Q water except for SMX, which was prepared in methanol. An intermediate SMX stock was prepared in water from the concentrated methanol stock. All experiments were conducted in triplicates, and samples were shaken on a Fisherbrand multipurpose tube rotator (Fisher Scientific, Waltham, MA) at 40 rpm.

The efficacy of the Fe(VI)-coated sand was evaluated in multiple contaminant systems and at different pH values (pH 7.5 and 9). These pH values were chosen to assess the Fe(VI)-coated sand reactivity when its aqueous stability is high (i.e., at pH 9) and at environmentally relevant pH (i.e., pH 7.5). A pH range of 6.5–8.5 is typical of wastewater effluent.^{40,41} Additionally, an assessment of pH effects on the aqueous stability of the Fe(VI)-coated sand demonstrated that the Fe(VI)-coated sand was more stable at pH 9, as reported in our previous publication.¹⁹ Batch kinetics experiments were conducted in four different reaction systems: (i) all three trace organics in a pH 9, 10 mM sodium borate buffer solution (**O9 system**); (ii) all three trace metals in a pH 9, 10 mM sodium borate buffer solution (**M9 system**); (iii) trace organics and metals together in a pH 9, 10 mM sodium borate buffer solution (**MO9 system**); and, (iv) trace organics and metals together in a pH 7.5, 10 mM sodium borate buffer solution (**MO7.5 system**). The concentration of the contaminants was targeted at 500 μg/L each, and the dose of the Fe(VI)-coated sand was 2 g/L for all reaction systems explored in this study. This dose (2 g/L) of Fe(VI)-coated sand was previously found to maximize removal of phenol.¹⁹ At designated time intervals, a 2 mL aliquot of samples containing the organic compounds was quenched with 20 μL of 500 mM Na₂SO₃ to stop

the reaction between Fe(VI) and the organic compounds and then filtered with a 0.2 μm , 25 mm-diameter cellulose acetate syringe filter before analysis using high-performance liquid chromatography (HPLC) methods (Text S2). Liquid chromatography-mass spectrometry (LC-MS) grade methanol (500 μL) was added to 500 μL of the quenched and filtered aliquot for high-resolution mass spectrometry (HRMS) analyses (Text S3) to determine transformation products of the organic compounds. For all samples, a 3 mL aliquot was taken and filtered with a 0.2 μm , 25 mm diameter cellulose acetate syringe filter, and then 1 mL of the aliquot was used to measure the aqueous Fe(VI) concentration via the 2,2'-azinobis(3-ethylbenzothiazoline-6-sulfonate) (ABTS) colorimetric method⁴² via UV-vis spectroscopy using a Shimadzu UV-2700 spectrophotometer (Kyoto, Japan). The remaining aliquot was diluted with a 10 mM sodium borate buffer solution and acidified to 2% trace metal grade nitric acid for inductively coupled plasma orbital mass spectrometry (ICP-MS) analysis using a PerkinElmer Nexion 2000B inductively coupled mass spectrometer (Waltham, MA).

Control experiments in the absence of the Fe(VI)-coated sand were conducted to assess the stability and reactivity of the trace metals and organics in solution for all four reaction systems. In addition, the role of Fe(III) phases in the Fe(VI)-coated sand reactivity was evaluated. A weighted amount (1.3 ± 0.1 mg) of Fe(NO₃)₃·9H₂O was added to 50 mL of either a pH 9, 10 mM sodium borate buffer solution or a pH 7.5, 10 mM sodium borate buffer solution containing all the trace metals and trace organics. The final Fe(III) concentration (26 ± 1.8 mg/L) in solution was chosen as an overestimate of the total Fe concentration (12.6 ± 5.1 mg/L) possible in solution if all of the Fe were to leach from the sand surface. At designated times, aliquots were taken and filtered prior to ICP-MS and HPLC analyses. The results from our previous study indicated that Fe(VI)-coated sand enhanced the removal and oxidation of phenol compared to application of Fe(VI) powder. Therefore, this study did not compare the treatment of the select contaminants with Fe(VI) powder.

2.4. Removal of Trace Metals and Organics in a Synthetic Wastewater Effluent Matrix

Batch kinetics experiments were also conducted under synthetic wastewater (SWW) effluent conditions to characterize the effects of the wastewater effluent matrix on the Fe(VI)-coated sand treatment capacity for the select trace contaminants. The matrix was prepared based on wastewater effluent (real and synthetic) compositions reported in the literature.^{40,43–46} The SWW composition included the following: NaHCO₃ (96 mg/L), NaCl (83 mg/L), MgCl₂·6H₂O (19 mg/L), Mg(NO₃)₂·6H₂O (10 mg/L), CaCl₂·2H₂O (89 mg/L), Ca(NO₃)₂·4H₂O (10 mg/L), and Na₂HPO₄ (1 mg/L). The detailed composition of the synthetic matrix is included in Table S4. Batch experiments were conducted by adding approximately 100 mg of Fe(VI)-coated sand in 50 mL of SWW in 50 mL polypropylene centrifuge tubes containing nominally 500 $\mu\text{g/L}$ of ACM, BZT, SMX, Cu, Pb, and Zn each. At designated time intervals, aliquots were sampled and analyzed as described in Section 2.3.

3. RESULTS AND DISCUSSION

3.1. Surface Analyses Confirm Fe Coating on the Sand Surface

SEM images indicate that Fe(VI) coating alters the surface morphology of the Ottawa sand (Figure 1). The unmodified Ottawa sand (Figure 1A) surface roughness increased following coating of the TeOS binder and the Fe(VI) (Figure 1B). Elemental analysis of the surface composition indicated mostly Si (32.5%) and O (54.5%) for the unmodified Ottawa sand (Figure 1), which confirms the expected high SiO₂ content of the sand structure.⁴⁷ The carbon detected on the Ottawa sand can be attributed to the carbon coating sample preparation done prior to analysis to reduce electrical charge on the nonconductive sand samples. On the Fe(VI)-coated sand surface, K (33.7%), Cl (1%), and Fe (1.7%) were

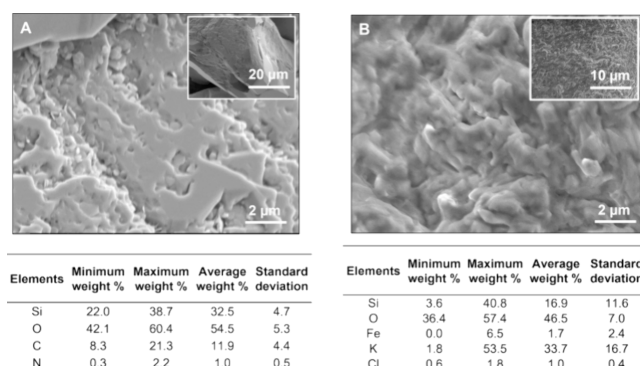


Figure 1. SEM images of (A) unmodified Ottawa sand and (B) Fe(VI)-coated sand. The insets are SEM images at lower magnification. The adjoining tables report elemental composition by weight percent on the medium surface.

detected, confirming the successful coating of potassium ferrate (K₂FeO₄).

The XRD analysis also confirmed Fe coating on the sand surface (Figure S2). An increase in the number of peaks was observed in the XRD pattern of the Fe(VI)-coated sand compared to the unmodified Ottawa sand and TeOS-coated sand, suggesting the presence of a new component (i.e., Fe(VI)) on the sand surface. Additional physicochemical characterization of the Fe(VI)-coated sand was performed in our previous study,¹⁹ which confirmed the presence of Fe(VI) on the sand surface.

3.2. In Situ Formation of Fe(III) Enhances the Removal of Trace Metals

The Fe(VI)-coated sand exhibited lower reactivity and removal efficiency toward the trace metals compared to trace organics. Furthermore, the reactivity toward Pb was greater than that of Cu and Zn. The batch adsorption results suggest that the trace metals are removed via interaction with Fe(III) particles generated during the reduction of leached Fe(VI) in the reaction solution (Figure 2 and Figure S3). For example, 100% removal of Pb and 94% removal of Zn (Figure S3A2) were observed after the 3 h reaction in the test evaluating Fe(III) removal capacity (i.e., Fe(III) solids only), whereas the Fe(VI)-coated sand treatment in the MO9 system only yielded 61% removal of Pb and 28% for Zn after 3 h reaction (Figure 2B). Additionally, the removal of Pb and Zn by Fe(VI)-coated sand was achieved at 23 and 26% in the M9 system in the absence of trace organics (Figure 2A). These data suggest that Fe(III) phases formed as a result of oxidation of trace organics and subsequent Fe(VI) reduction can increase Pb and Zn removal. At pH 9, Fe(VI) is stable and reacts slowly with water to form Fe(III),¹⁹ but this reduction can be accelerated in the presence of organic compounds reacting with and reducing Fe(VI). This is evidenced by the slower decrease in aqueous Fe(VI) concentrations seen in the M9 system (Figure S4A) compared to the faster decrease in the O9 system (Figure S4B) and MO9 systems (Figure S4C) when trace organics are present. The enhanced removal of metals in the presence of organic compounds validates the multifunctional properties of Fe(VI)-coated sand as an oxidant and coagulant.

Visual MINTEQ analysis suggests that Pb removal is governed by its chemical speciation in solution. In the pH 9, 10 mM borate buffer, Visual MINTEQ analysis indicates that Pb(OH)₂ is oversaturated in solution (Table S2B), which

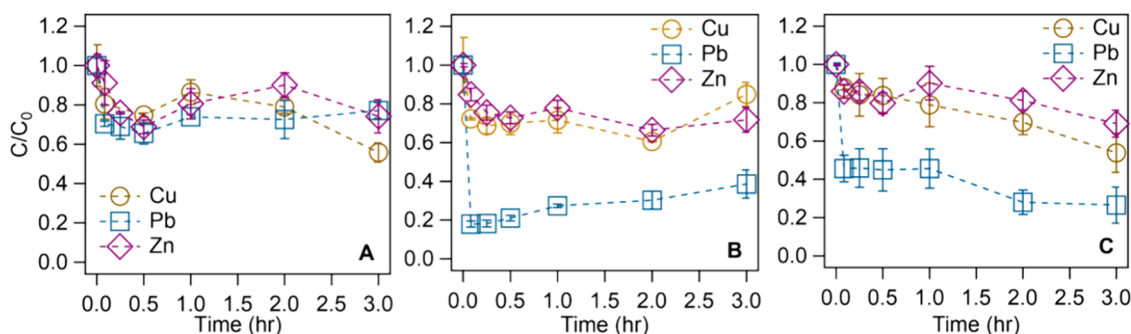


Figure 2. Removal of nominally 500 $\mu\text{g/L}$ Cu, Pb, and Zn (each) by 2 g/L Fe(VI)-coated sand (A) in the **M9** system and in the presence of nominally 500 $\mu\text{g/L}$ ACM, BZT, and SMX (each) (B) in the **MO9** system and (C) **MO7.5** system.

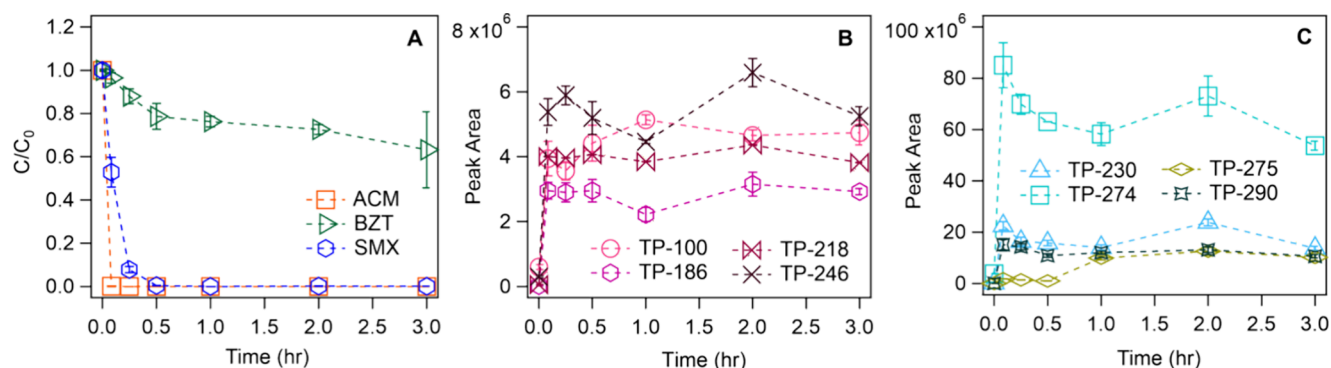


Figure 3. (A) Normalized degradation of nominally 500 $\mu\text{g/L}$ ACM, BZT, and SMX (each) by 2 g/L Fe(VI)-coated sand in the **O9** system and (B, C) formation of the most abundant transformation products (TP) as a function of time.

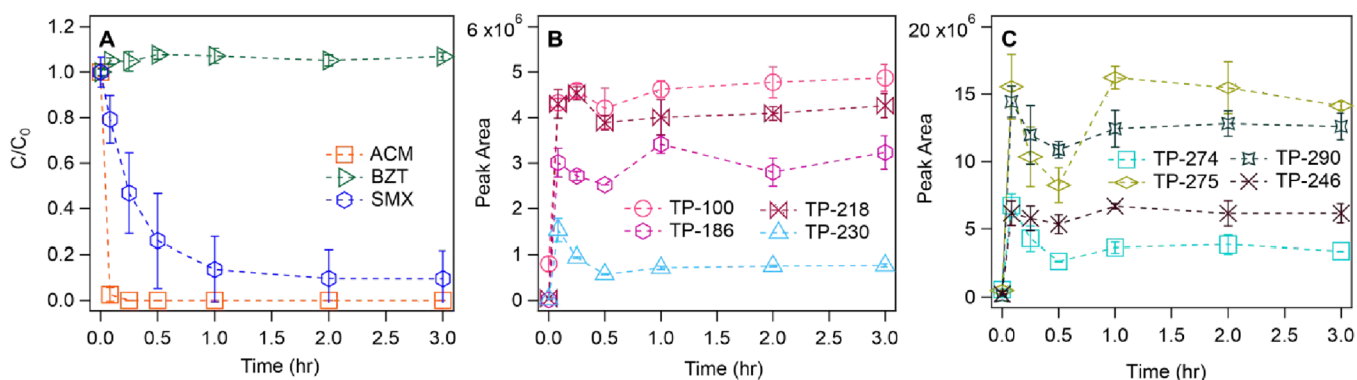


Figure 4. (A) Normalized degradation of nominally 500 $\mu\text{g/L}$ ACM, BZT, and SMX by 2 g/L Fe(VI)-coated sand in the **MO9** system in the presence of nominally 500 $\mu\text{g/L}$ Cu, Pb, and Zn (each) and (B, C) formation of the most abundant transformation products (TPs) as a function of time.

could contribute to precipitate formation. In the **M9** control samples (i.e., no Fe(VI)-coated sand), the removal of Pb after 3 h was 1.6 times greater than in the **M9** system. Thus, we hypothesize that the removal of Pb within the pH 9, 10 mM borate buffer system was predominantly facilitated by sample filtration of precipitates prior to ICP-MS measurements. We further posit that processes governing trace metal removal in our treatment systems could be 3-fold: (1) removal via filtration of solid phase precipitates formed due to oversaturation, (2) sorption to aqueous Fe(III) phases generated during reduction of leached aqueous Fe(VI), and (3) sorption onto the Fe-coated sand surface.

Trace metal removal by the Fe(VI)-coated sand decreased as pH decreased, especially in the case of Zn. Previous studies have reported an increase in metal removal by Fe(VI) as pH

increases due to favorable electrostatic interactions between the trace metals and in situ generated Fe(III) phases.^{13,48} The same trend was observed in our study (Figure 2). In the **MO7.5** system, the removal efficiencies of Zn and Pb decreased by 7 and 14% compared to removal in the **MO9** system. The isoelectric point of Fe(III) (hydr)oxide species is between pH 7 and 8.5;⁴⁹ thus, we hypothesize that at pH 9, the removal of Pb is driven by electrostatic interactions of the abundant $\text{Pb}(\text{OH})^+$ species (Table S2A) and the negatively charged Fe(III) (hydr)oxide surfaces. Furthermore, at pH 9, Fe(VI) exists predominantly as FeO_4^{2-} (Figure S1),^{19,50} which could also interact electrostatically with $\text{Pb}(\text{OH})^+$ species. In the case of Zn, the abundant species at pH 9 is $\text{Zn}(\text{OH})_2$, suggesting removal via physical sorption of Zn either on the media surface or within Fe(III) (hydr)oxide lattices.

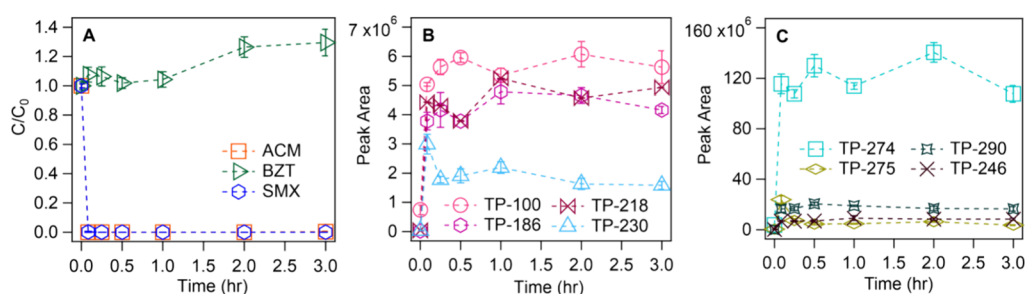


Figure 5. (A) Normalized degradation of nominally 500 $\mu\text{g/L}$ ACM, BZT, and SMX (each) by 2 g/L Fe(VI)-coated sand in the MO7.5 system in the presence of nominally 500 $\mu\text{g/L}$ Cu, Pb, and Zn (each) and (B, C) formation of the most abundant transformation products (TPs) as a function of time.

Conversely, at pH 7.5, Pb^{2+} and Zn^{2+} are the more abundant species and may sorb weakly to the neutral Fe(III) (hydr)oxide surface. The pH effect on metal removal in the Fe(VI)-coated sand treatment systems is also mirrored in the Fe(III) reaction systems (Figure S3). After the 3 h reaction with Fe(III), the removal of Zn increased from 31% at pH 7.5 to 94% at pH 9 (Figure S3A1,A2).

Interestingly, Cu removal was greater in the control experiments in the absence of Fe(VI)-coated sand, regardless of solution pH (Figure S5). Visual MINTEQ analysis reports CuO and Cu(OH)₂ as the oversaturated mineral phases present in solution; thus, the high removal efficiencies observed in the control samples could be attributed to the formation of these mineral phases, which were removed during filtration. Furthermore, greater Cu removal efficiencies were achieved in the MO7.5 and MO9 control systems. For example, the presence of trace organics in the MO9 control system led to a 58% increase in Cu removal, which suggests that Cu is interacting with the trace organics (discussed in more detail in Section 3.3).

3.3. Solution pH and Composition Affect Degradation of Trace Organics

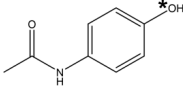
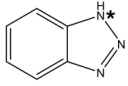
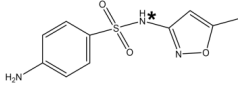
Fe(VI)-coated sand exhibited a greater oxidation potential toward ACM and SMX compared to BZT. Figures 3–5 indicate the oxidation of the three select trace organics in this study by the Fe(VI)-coated sand and their corresponding transformation products identified using HRMS. For all of the test reaction systems, the degradation of ACM was complete and occurred rapidly (within 15 min, Figures 3–5). Oxidation efficiencies of 100% were achieved for SMX in the O9 (Figure 3) and MO7.5 reaction systems (Figure 5), and 90% oxidation was achieved in the MO9 system (Figure 4) after the 3 h reaction. For BZT, the oxidation efficiency was 37% in the O9 system (Figure 3), but no removal was detected in the MO9 system and MO7.5 system (Figures 4 and 5). The greater removal of ACM and SMX can be attributed to the high Fe(VI) selectivity toward electron-donating moieties such as phenols (present in ACM) and anilines (present in SMX).^{16,29}

The solution matrix and pH were found to influence the oxidation potential of ACM and SMX by the Fe(VI)-coated sand. The presence of trace metals in the MO9 system led to a 26% decrease in SMX oxidation capacity within 5 min of reaction compared to oxidation in the O9 system (i.e., absence of trace metals) (Figures 3A and 4A). The SMX oxidation capacity increased from 21% at pH 9 (Figure 4A, MO9 system) to 100% at pH 7.5 (Figure 5A, MO7.5 system) within 5 min of reaction. This difference can be explained by the differences in Fe(VI) chemical speciation at pH 7.5 compared

to pH 9 (Figure S1). At pH 7.5, Fe(VI) is comprised of 38.7% HFeO_4^- and 61.3% FeO_4^{2-} .¹⁹ HFeO_4^- species are reported to have a higher oxidation potential than FeO_4^{2-} species,^{51,52} which may result in greater degradation of ACM and SMX at pH 7.5. At pH 9, the degradation of the trace organics decreased (Figure 4A), which could be due to three effects: (1) the less reactive FeO_4^{2-} species is dominant at this pH (i.e., 98%, Figure S1); (2) the presence of more contaminants in solution result in greater competition for reactions with Fe(VI); and, (3) Fe(VI) decays to intermediate and Fe(III) phases faster when there are more contaminants present. Results of aqueous Fe(VI) concentration evolution show that Fe(VI) decays faster in the MO9 and MO7.5 reaction systems containing all contaminants (Figure S4C) compared to the systems containing one type of contaminant (Figure S4B). To enhance the decomposition of trace organics during wastewater treatment with more complex matrices containing multiple contaminant types, higher doses of Fe(VI)-coated sand or higher Fe(VI) mass loadings on the sand surface may be required. However, we note that within the 3 h reaction period used in this study, removal efficiencies of 90% or greater were still achieved for ACM and SMX despite the mass of contaminants present.

BZT complexation with Cu inhibits its treatment by the Fe(VI)-coated sand. BZT is used as a corrosion inhibitor for Cu^{53,54} and has been reported to form metal complexes with Cu⁺ and Cu²⁺ through electron transfer between the BZT nitrogen atoms.^{55,56} The formation of Cu–BZT complexes has been leveraged in some studies to enhance BZT degradation in wastewater. For example, Zhang et al. investigated the use of a mesoporous Cu/MnO₂ composite to catalyze oxidation of BZT by hydrogen peroxide.⁵³ The oxidation of BZT by MnO₂ was facilitated by the Cu–BZT complex formed on the catalyst surface.⁵³ However, in our study, the presence of Cu did not enhance BZT degradation (Figures 4 and 5). In the O9 system, we observed up to 37% removal of BZT after 3 h of reaction (Figure 3A); however, in the MO9 system and MO7.5 systems containing metals, we observed an artificial increase in the measured aqueous BZT concentrations (Figure 4A and 5A). The increase was higher for the pH 7.5 condition after 2 h of reaction. Furthermore, results from the control experiments (i.e., absence of media) for the MO9 system and MO7.5 system (Figure S6B–D) and the test performed in the presence of Cu only (Figure S7) indicate a decrease in measured BZT concentrations (Figure S6B–D) (Figure S7), which suggests the formation of the Cu–BZT complex. Cu–BZT complexes are reported to be insoluble in water;⁵⁵ thus, we hypothesize that the Cu–BZT complexes formed in our systems are removed via filtration prior to HPLC analysis,

Table 1. Structures and Properties of Select Trace Organic Compounds and Metals Used in This Study^{35–39a}

trace organic compounds	sources	structure	pKa	Log K _{ow}
acetaminophen (ACM)	analgesic drug (Zhang et al. ³⁵)		9.71 (Li et al. ²⁸)	0.46 (Snyder et al. ³⁶)
benzotriazole (BZT)	anti-corrosion agent, UV-inhibitors (Mawhinney et al. ³³)		pKa ₁ = 1.6 pKa ₂ = 8.6 (Xu et al. ³⁷)	1.23 (Hart et al. ³⁸)
sulfamethoxazole (SMX)	antimicrobial drug (Dodd et al. ³⁰)		pKa ₁ = 1.7 pKa ₂ = 5.6 (Dodd et al. ³⁰)	0.89 (Snyder et al. ³⁶)
trace metals	sources	matrix pH	speciation	% abundance
copper	fertilizers, paints, oil refining, mining (Khan et al. ⁴)	9	Cu(OH) ₂ (aq) (<i>Cu(OH)₂(s)</i> , <i>CuO(am, c)</i>)	57.1
		7.5	Cu ²⁺ CuOH ⁺ (<i>CuO(am, c)</i>)	46.1 45.6
lead	lead-based batteries, paints (Chowdhury et al. ³⁹); fertilizers (Das et al. ³)	9	Pb(OH) ⁺ (<i>Pb(OH)₂(s)</i>)	73.5
		7.5	Pb ²⁺ (<i>Pb(OH)₂(s)</i>)	55.7
zinc	oil refining, textiles, rubber products (Das et al. ⁵)	9	Zn(OH) ₂ (aq) (<i>ZnO</i>)	86.0
		7.5	Zn ²⁺	95.8

^aThe asterisks (*) on the structures show the moieties that can be deprotonated or protonated at the pH values used in this study. The mineral phases in italics are the oversaturated mineral phases for the metal species as determined by Visual MINTEQ at the given pH.

which explains the lower concentrations obtained in the control experiments described above (Figures S6B–D and S7). The Cu–BZT complexation is also made evident in the measured aqueous concentrations of Cu in the control experiments conducted in the absence of media (Figure S5). For example, in the M9 control system, 36% Cu removal was observed; however, in the MO9 control system, 98% Cu was removed after 3 h of reaction in the presence of BZT and the other trace organics. We hypothesize that the reaction between the Cu–BZT complexes and the Fe(VI)-coated sand media leads to the decomplexation of Cu–BZT and the release of aqueous Cu and BZT into solution. Previous studies have reported the successful removal of metal complexes by Fe(VI).^{48,57–59} For example, Tiwari et al.⁵⁹ investigated the removal of iminodiacetic acid (IDA) complexes with Cu(II), Ni(II), and Cd(II) at pH 8, 9, and 10. They reported a removal efficiency of up to 80% of total organic carbon when the concentrations of Cd(II)-IDA and Ni(II)-IDA were 0.3 mM.⁵⁹ The removal of the metal complexes in their study was hypothesized to be initiated by the decomplexation by Fe(VI) followed by oxidation of IDA.⁵⁹ Further removal of the freed metals by Fe(VI) was also reported.⁵⁹ In this study, while we observed the decomplexation of the Cu–BZT complex as evidenced by the increase in aqueous BZT concentration, the free BZT did not react further with Fe(VI). This could be due to the lesser Fe(VI) affinity toward BZT, which is observed in Figure 3. Further investigations with higher doses of the Fe(VI)-coated sand media or lower concentrations of

contaminants will be explored to determine whether the decoupled BZT could be degraded when there is more Fe(VI) available in solution.

3.4. Trends in Transformation Product Formation Validates Oxidation Mechanisms of the Trace Organics

HRMS results were analyzed as described in Text S3. Based on this analysis, 85 transformation products (TPs) were identified in the O9 system (Table S5), 46 TPs in the MO9 system (Table S6), and 72 TPs in the MO7.5 system (Table S7). The lower number of TPs detected in the trace metal-containing systems supports the findings discussed in Section 3.3 when a decrease in oxidation efficiency of the trace organics in the presence of metals was observed. We recognize that the large pool of TPs detected could be due to the inclusion of multiple fragments from the same parent compounds and additional steps are needed to further isolate the transformation products. However, we note that the primary objective of this study is to assess the reactivity of the Fe(VI)-coated sand media in complex matrices; therefore, further analyses were not conducted to identify the structures of the TPs nor to deduct oxidation pathways for all TPs generated. Some proposed oxidation pathways, however, are discussed later in this section.

The higher peak areas observed for TPs in the O9 and MO7.5 systems corroborate the observed solution pH and matrix effects on the oxidation efficiency of the trace organics by the Fe(VI)-coated sand. While over 40 TPs were identified in reaction systems containing trace organics, eight TPs were portrayed in Figures 3–5 because they were formed at the

highest yield: TP-100, TP-186, TP-218, TP-230, TP-246, TP-274, TP-275, and TP-290 (Figures 3–5). For all eight featured TPs, we observed a sharp increase (by 2 orders of magnitude or greater) in peak area after 5 min of reaction, which confirms the fast reactivity of the Fe(VI)-coated sand toward the trace organics. Additionally, all the featured TPs except for TP-230 and TP-275 exhibited an increase in peak area at pH 7.5 (Figure 5B,C), emphasizing the greater reactivity of Fe(VI) at pH 7.5 due to the HFeO_4^- species. However, for TP-230, we observed more than an 85% decrease in peak area in the presence of trace metals at both pH values (Figures 4B and 5B). Furthermore, the maximum peak area for TP-230 was obtained in the presence of the trace metals (in the MO9 system and MO7.5 system) at 5 min of reaction, which indicates that TP-230 formed within 5 min of treatment and then subsequently decreased. These results suggest that the presence of trace metals inhibits the formation of TP-230 or that the trace metals react with TP-230 to form metal complexes. Additionally, the TP-275 peak area after 5 min of reaction in the MO7.5 system was 35% greater than the peak area in the MO9 system; however, after 3 h of reaction, the peak area in the MO7.5 system was 74% less than the peak areas in the MO9 system. This implies that the formation of TP-275 is a pH-dependent reaction and that TP-275 may be undergoing reactions with the trace metals.

In the MO9 system and MO7.5 system, BZT oxidation did not occur, suggesting that TP-275 is a transformation product of either ACM or SMX. Furthermore, under pH 7.5 and 9 conditions, SMX is deprotonated, whereas ACM is protonated (see Table 1). Thus, we hypothesize that TP-275 is a transformation product of SMX that can react with the positively charged metal species via electrostatic interactions. In particular, at pH 7.5 in the MO7.5 system, Cu, Pb, and Zn exist predominantly as Cu^{2+} , Pb^{2+} , and Zn^{2+} (Table S3A), respectively; thus, complexation between these cations and a negatively charged TP may explain the significant decrease in the TP-275 peak area in the MO7.5 system. Future work will be performed to identify these compounds and elucidate their fate in our treatment systems.

Comparing the trends in the TP yields with the measured oxidation efficiencies of the trace organics suggests that TP-100, TP-186, TP-218, and TP-246 are potential oxidation products of ACM, whereas TP-274 and TP-290 may be oxidation products of SMX. While we recorded a slight increase in peak area at pH 7.5 for TP-100, TP-186, TP-218, and TP-246 (Figure 5), their peak areas were relatively similar across the test reaction systems (i.e., O9, MO9, and MO7.5 in Figures 3B, 4B, and 5B, respectively). For example, the peak areas for TP-218 after 3 h of reaction were 3.82×10^6 in the O9 system, 4.26×10^6 in the MO9 system, and 4.94×10^6 in the MO7.5 system. The consistent formation of these TPs at similar quantities aligns with the comparable oxidation capacity observed for ACM across the three reaction systems containing trace organics (Figures 3A–5A). Oxidation of organic compounds by Fe(VI) occurs via electrophilic attack of electron-rich moieties (e.g., phenols, amines, anilines, and olefins).^{25,60,61} Thus, we hypothesize that Fe(VI) oxidation of ACM and SMX will occur with their phenolic and aniline moieties, respectively. For ACM, oxidation could proceed by separation of the amide moiety and phenol moiety followed by cleavage of the latter⁶² to produce TP-100 (Figure S8). Additionally, oxidation of ACM could occur via hydrolysis. In neutral to alkaline solutions, Fe(VI) reacts with water to form

$\text{Fe}(\text{OH})_3$ and OH^- .⁶³ We suspect that the formation of OH^- could enhance the hydrolysis of ACM at the benzene ring⁶² to produce TP-186 (Figure S8). Conversely, the chemical structure of SMX can contribute to multiple oxidation pathways for reaction with Fe(VI), which can happen via the aniline group, the isoxazole group, or at the N–S bond (Figure S9).^{16,64} The hypothesized SMX TP-274 peak area decreased by 94% in the MO9 system compared to the O9 system after 3 h of reaction. At environmental pH (i.e., the MO7.5 system), the TP-274 peak area increased by 50% compared to the peak area in the O9 system. The observed trends with respect to peak area magnitude correspond with the trends in SMX oxidation observed in the MO9 (Figure 4A) and MO7.5 (Figure 5A) reaction systems. Furthermore, the literature reports an oxidation product with a mass:charge (m/z) value of 276 during the oxidation of SMX by Fe(VI).^{64,65} We hypothesize that the TP-274 detected in our study is similar to this oxidation product reported in the literature. The formation of this transformation product occurs through the cleavage and subsequent hydroxylation of the isoxazole moiety in SMX^{64,66} (Figure S9). It is further degraded via hydroxylation of the benzene ring to form a product with a reported m/z value of 292.^{64,66} We attribute this compound to TP-290 identified in our study (Figure S9).

3.5. Wastewater Effluent Constituents Inhibit Trace Organic Oxidation but Promote Trace Metal Sorption

Trace organic oxidation by Fe(VI)-coated sand is lessened in the synthetic wastewater reaction system. After 3 h of reaction with the media, only 7.24% removal of SMX was achieved (Figure 6A). While the oxidation efficiency of ACM remained

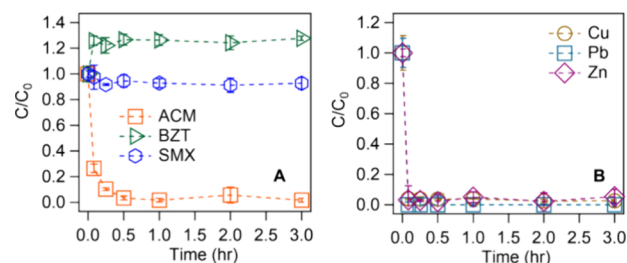


Figure 6. Removal of nominally 500 $\mu\text{g/L}$ (each) (A) ACM, BZT, and SMX and (B) Cu, Pb, and Zn by 2 g/L Fe(VI)-coated sand in a synthetic wastewater effluent solution as a function of time.

high (98.4%) (Figure 6A), the degradation was slower in SWW compared to degradation in the borate buffer solutions (Figures 3–5). Oxidation of BZT in the SWW was minimal, and as before, we observed an artificial increase in the aqueous BZT concentration during the reaction period (Figure 6A). While some studies have reported no effect of inorganic ions (i.e., Na^+ , Ca^{2+} , Cl^- , and HCO_3^-) on Fe(VI) oxidation capacity,^{25,67} others have noted that the presence of these ions will impede ferrate oxidation.^{68,69} For example, Feng et al. observed a 10% decrease in flumequine oxidation by Fe(VI) in the presence of Ca^{2+} and Mg^{2+} ions,⁶⁹ which was attributed to the catalytic effects of these cations on the self-decomposition of Fe(VI) in solution.^{69,70} Specifically, Ma et al. investigated the effect of Ca^{2+} on Fe(VI) decomposition at pH 9–10 and demonstrated that Ca^{2+} bridges FeO_4^{2-} ions to facilitate the formation of the diferrate intermediate,⁷⁰ which undergoes reduction to produce Fe(III).^{70,71} The same effect is expected for other divalent ions present in the synthetic wastewater

matrix (i.e., Mg^{2+}).⁷⁰ In the SWW treatment system, Fe(VI) consists of predominantly FeO_4^{2-} ions (83.4%); thus, we suspect that the Ca^{2+} and Mg^{2+} ions present will react with FeO_4^{2-} to catalyze Fe(VI) decomposition and decrease the oxidation of ACM and SMX.

Conversely, the SWW constituents enhanced trace metal removal by the Fe(VI)-coated sand. Greater (>94%) and faster (within 5 min of reaction) removal efficiencies were recorded for all three trace metals in the SWW reaction system (Figure 6B) compared to the treatment systems in borate buffer. While the removal of Cu and Pb can be partially attributed to the removal of solid phases through filtration, the removal of Zn is completely achieved by the media. In the SWW control samples in the absence of Fe(VI)-coated sand, Zn removal did not occur (Figure S4D); however, the presence of the media led to a 94.7% removal of Zn in SWW (Figure 6B). Therefore, while the self-decomposition of Fe(VI) by the Ca^{2+} and Mg^{2+} ions hindered transformation of trace organics within the SWW matrix, the faster generation of Fe(III) species in solution promoted trace metal removal. However, we observed that the total mass of leached, aqueous Fe(VI) in the SWW reaction system (Figure S7) was comparable to the leached mass in the MO9 system (Figure S6C), indicating that the effect of Ca^{2+} and Mg^{2+} might be limited to interferences with oxidative processes in our treatment systems.

The decreased oxidation efficiency of trace organics coupled with the enhanced removal of trace metals in the SWW matrix suggests a hierarchy in Fe(VI) reactivity toward contaminants and coexisting ions. The significant difference in ACM and SMX oxidation efficiencies (Figure 6A) in the SWW matrix (91%) compared to the difference in the oxidative removal of ACM and SMX in the MO9 system (10%) and MO7.5 system (no difference) demonstrates preferential affinity of the Fe(VI)-coated sand for ACM. Furthermore, the diminished oxidation efficiency of SMX and BZT in the SWW matrix indicates that Fe(VI) favorably reacts with hydrophilic and protonated ACM, divalent cations, and water molecules in the SWW system. Additionally, these three interactions boost formation of Fe(III) phases to significantly improve trace metal removal. These results further demonstrate the promising potential for Fe(VI)-coated sand for the treatment of contaminants in complex matrices.

4. CONCLUSIONS

The Fe(VI)-coated sand composite media proved to be a highly effective treatment for Fe(VI) deployment in water treatment applications. The effect of water chemistries (i.e., pH and inorganic ions) and matrix complexity (i.e., multiple contaminants) on the reactivity of the Fe(VI)-coated sand was explored through batch tests. Treatment of ACM, SMX, BZT, Cu, Pb, and Zn at equal initial concentrations revealed that Fe(VI) had a greater affinity for the trace organics, especially for ACM for which removal efficiency exceeded 90% under all experimental conditions tested. The presence of Cu in the treatment systems inhibited BZT removal due to the formation of Cu–BZT complexes. Therefore, if such complexes form in solution during application of Fe(VI)-coated sand, treatment of both complex components may be compromised. A faster removal of ACM and SMX was achieved at pH 7.5 compared to pH 9, indicating that the lower environmental pH is favorable for trace organic oxidation due to the increased presence of HFeO_4^- ions in solution. The removal of ACM and SMX decreased at pH 9 in the presence of trace organics

and at pH 8 in the presence of trace metals and inorganic ions, suggesting that at pH values where HFeO_4^- ions exist in smaller quantities, the removal of trace organics may depend on the ratio of Fe(VI) species to contaminants. HRMS results indicated that the removal of trace organics occurred via oxidation. Sharp increases (by 2 or more orders of magnitude) in peak areas of the observed transformation products occurred within 5 min of reaction which validates the high reactivity of the media toward the trace organics. While Cu and Pb removal was partially attributed to the removal of their mineral solid phases, Zn removal occurred solely via interaction with the Fe(VI)-coated sand. Thus, the increased removal of Zn in the presence of trace organics indicated that trace metal removal was achieved by Fe(III) formed in solution after Fe(VI) reaction with the trace organics.

This study demonstrates the potential of Fe(VI)-coated sand media for the treatment of multiple contaminants in complex matrices, such as in wastewater effluents. Here, we used concentrations that are higher than typical concentrations of trace organics and trace metals in the environment. We expect, as with any chemical oxidant and coagulant, that 100% removal or degradation of all contaminant types will not be achieved. Therefore, our goal was not to optimize the Fe(VI)-coated sand for contaminant remediation but rather to evaluate its viability as treatment a media. Future work exploring the treatment capabilities of the Fe(VI)-coated sand will probe the removal of contaminants at environmentally relevant concentrations as well as in the presence of dissolved organic carbon to better assess the Fe(VI)-coated sand capacity for treatment. Additionally, we will also assess Fe(VI)-coated sand performance during column studies to mimic real-world treatment systems.

■ ASSOCIATED CONTENT

SI Supporting Information


The Supporting Information is available free of charge at <https://pubs.acs.org/doi/10.1021/acsenvironau.4c00024>.

Chemicals and materials used; description of analysis methods used for HPLC and HRMS data; Visual MINTEQ analyses; synthetic wastewater effluent solution composition; chemical speciation and decay constant of Fe(VI); XRD patterns of the noncoated sand, TeOS-sand, Fe(VI) powder, and Fe(VI)-coated sand; results of control experiments in the presence of $\text{Fe}(\text{NO}_3)_3 \cdot 9\text{H}_2\text{O}$ and in the absence of media; measurements of aqueous Fe(VI) concentrations during treatment of contaminants; results of control experiments with Cu and BZT in the absence of media; oxidation pathways of ACM and SMX; tables of transformation products obtained via HRMS data (PDF)

All prioritized TPs from oxidation of organics by Fe(VI)-coated sand at pH 9 in the absence of trace metals, at pH 9 in the presence of trace metals, and at pH 7.5 in the presence of trace metals (XLSX)

■ AUTHOR INFORMATION

Corresponding Author

Jessica R. Ray – Department of Civil & Environmental Engineering, University of Washington, Seattle, Washington 98195-2700, United States;  orcid.org/0000-0002-9964-3799; Email: jessray@uw.edu

Authors

Fanny E. K. Okaikue-Woodi – Department of Civil & Environmental Engineering, University of Washington, Seattle, Washington 98195-2700, United States

Reyna Morales Lumagui – Department of Chemical Engineering, University of Washington, Seattle, Washington 98195-2700, United States

Complete contact information is available at:

<https://pubs.acs.org/10.1021/acsenvironau.4c00024>

Author Contributions

The manuscript was written through contributions of all authors. All authors have given approval to the final version of the manuscript. F.E.K.O.-W.: conceptualization, experimentation, methodology, data analysis, writing, and editing; R.M.L.: experimentation, methodology, and writing; J.R.R.: conceptualization, funding acquisition, writing, and editing.

Funding

This research was supported by the National Science Foundation (CBET 2242483) as well as by funds from the University of Washington.

Notes

The authors declare no competing financial interest.

ACKNOWLEDGMENTS

We would like to thank Dr. Michael C. Dodd for the use of the VWR recirculating chiller needed for the Fe(VI)-coated sand synthesis. We would also like to thank Reagan Beers for assistance with XRD data collection and analyses. We would like to thank Dr. Ed Kolodziej at the Center for Urban Waters (Tacoma, WA) for the use of the QTOF-HRMS used for oxidation product analysis, and Dr. Ximin Hu for assistance with the HRMS data collection and analysis. The QTOF-HRMS analyses were possible due to the NSF MRI program funding (Grant 2117239). Part of this work was conducted at the Molecular Analysis Facility, a National Nanotechnology Coordinated Infrastructure (NNCI) site at the University of Washington with partial support from the National Science Foundation via awards NNCI-2025489 and NNCI-1542101. We would also like to thank Dr. Scott Braswell for assistance with SEM imaging and EDS analyses, and Dr. Mike De Sienna for assistance with the ICP-MS analyses.

REFERENCES

(1) Asano, T. *Water reuse: issues, technologies, and applications*; McGraw-Hill, 2007.

(2) Kolpin, D. W.; Furlong, E. T.; Meyer, M. T.; Thurman, E. M.; Zaugg, S. D.; Barber, L. B.; Buxton, H. T. Pharmaceuticals, Hormones, and Other Organic Wastewater Contaminants in U.S. Streams, 1999–2000: A National Reconnaissance. *Environ. Sci. Technol.* **2002**, *36* (6), 1202–1211.

(3) Luo, Y.; Guo, W.; Ngo, H. H.; Nghiem, L. D.; Hai, F. I.; Zhang, J.; Liang, S.; Wang, X. C. A review on the occurrence of micropollutants in the aquatic environment and their fate and removal during wastewater treatment. *Sci. Total Environ.* **2014**, *473–474*, 619–641.

(4) Khan, J.; Lin, S.; Nizeyimana, J. C.; Wu, Y.; Wang, Q.; Liu, X. Removal of copper ions from wastewater via adsorption on modified hematite (α -Fe₂O₃) iron oxide coated sand. *J. Cleaner Prod.* **2021**, *319*, No. 128687.

(5) Das, T. K.; Poater, A. Review on the Use of Heavy Metal Deposits from Water Treatment Waste towards Catalytic Chemical Syntheses. *Int. J. Mol. Sci.* **2021**, *22* (24), 13383.

(6) Bakare, B. F.; Adeyinka, G. C. Evaluating the Potential Health Risks of Selected Heavy Metals across Four Wastewater Treatment Water Works in Durban, South Africa. *Toxics* **2022**, *10* (6), 340.

(7) Baquero, F.; Martinez, J. L.; Canton, R. Antibiotics and antibiotic resistance in water environments. *Curr. Opin. Biotechnol.* **2008**, *19* (3), 260–265.

(8) Lindqvist, N.; Tuhkanen, T.; Kronberg, L. Occurrence of acidic pharmaceuticals in raw and treated sewages and in receiving waters. *Water Res.* **2005**, *39*, 2219–2228.

(9) Kummerer, K. Antibiotics in the aquatic environment – A review – Part I. *Chemosphere* **2009**, *75*, 417–434.

(10) Ferrari, B.; Paxéus, N.; Giudice, R. L.; Pollio, A.; Garric, J. Ecotoxicological impact of pharmaceuticals found in treated wastewaters: study of carbamazepine, clofibrac acid, and diclofenac. *Ecotoxicol. Environ. Saf.* **2003**, *56* (3), 450.

(11) Sharma, V. K. Potassium ferrate(VI): an environmentally friendly oxidant. *Adv. Environ. Res.* **2002**, *6* (2), 143–156.

(12) Jiang, J.-Q.; Lloyd, B. Progress in the Development and Use of Ferrate(VI) Salts as an Oxidant and Coagulant for Water and Wastewater Treatment. *Water Res.* **2002**, *36*, 1397–1408.

(13) Prucek, R.; Tucek, J.; Kolarik, J.; Huskova, I.; Filip, J.; Varma, R. S.; Sharma, V. K.; Zboril, R. Ferrate(VI)-prompted removal of metals in aqueous media: mechanistic delineation of enhanced efficiency via metal entrenchment in magnetic oxides. *Environ. Sci. Technol.* **2015**, *49* (4), 2319–2327.

(14) Jiang, J.-Q.; Wang, S.; Panagouloupoulos, A. The exploration of potassium ferrate(VI) as a disinfectant/coagulant in water and wastewater treatment. *Chemosphere* **2006**, *63* (2), 212–219.

(15) Fan, J.; Lin, B.-H.; Chang, C.-W.; Zhang, Y.; Lin, T.-F. Evaluation of potassium ferrate as an alternative disinfectant on cyanobacteria inactivation and associated toxin fate in various waters. *Water Res.* **2018**, *129*, 199–207.

(16) Yang, B.; Ying, G.-G.; Zhao, J.-L.; Liu, S.; Zhou, L.-J.; Chen, F. Removal of selected endocrine disrupting chemicals (EDCs) and pharmaceuticals and personal care products (PPCPs) during ferrate(VI) treatment of secondary wastewater effluents. *Water Res.* **2012**, *46* (7), 2194–2204.

(17) Wood, R. H. The Heat, Free Energy and Entropy of the Ferrate(VI) Ion. *J. Am. Chem. Soc.* **1958**, *80* (9), 2038–2041.

(18) Hao, L.; Liu, M.; Wang, N.; Li, G. A critical review on arsenic removal from water using iron-based adsorbents. *RSC Adv.* **2018**, *8* (69), 39545–39560.

(19) Okaikue-Woodi, F. E. K.; Ray, J. R. Synthesis of ferrate (Fe(vi))-coated sand for stabilized reactivity and enhanced treatment of phenol. *J. Mater. Chem. A* **2023**, *11*, 13552–13563.

(20) Feng, M.; Cizmas, L.; Wang, Z.; Sharma, V. K. Activation of ferrate(VI) by ammonia in oxidation of flumequine: Kinetics, transformation products, and antibacterial activity assessment. *Chem. Eng. J.* **2017**, *323*, 584–591.

(21) Feng, M. B.; Cizmas, L.; Wang, Z. Y.; Sharma, V. K. Synergistic effect of aqueous removal of fluoroquinolones by a combined use of peroxydisulfate and ferrate(VI). *Chemosphere* **2017**, *177*, 144–148.

(22) Manoli, K.; Li, R.; Kim, J.; Feng, M.; Huang, C.-H.; Sharma, V. K. Ferrate(VI)-peracetic acid oxidation process: Rapid degradation of pharmaceuticals in water. *Chem. Eng. J.* **2022**, *429*, No. 132384.

(23) Manoli, K.; Nakhla, G.; Ray, A. K.; Sharma, V. K. Enhanced oxidative transformation of organic contaminants by activation of ferrate(VI): Possible involvement of Fe(V)/Fe(IV) species. *Chem. Eng. J.* **2017**, *307*, 513–517.

(24) Tian, S.-Q.; Wang, L.; Liu, Y.-L.; Ma, J. Degradation of organic pollutants by ferrate/biochar: Enhanced formation of strong intermediate oxidative iron species. *Water Res.* **2020**, *183*, No. 116054.

- (25) Manoli, K.; Nakhla, G.; Feng, M.; Sharma, V. K.; Ray, A. K. Silica gel-enhanced oxidation of caffeine by ferrate(VI). *Chem. Eng. J.* **2017**, *330*, 987–994.
- (26) Sharma, V. K.; O'Connor, D. B.; Cabelli, D. E. Sequential One-Electron Reduction of Fe(V) to Fe(III) by Cyanide in Alkaline Medium. *J. Phys. Chem. B* **2001**, *105* (46), 11529–11532.
- (27) Harada, H.; Kurauchi, M.; Hayashi, R.; Eki, T. Shortened lifespan of nematode *Caenorhabditis elegans* after prolonged exposure to heavy metals and detergents. *Ecotoxicol. Environ. Saf.* **2007**, *66* (3), 378–383.
- (28) Li, Y.; Song, W.; Fu, W.; Tsang, D. C. W.; Yang, X. The roles of halides in the acetaminophen degradation by UV/H₂O₂ treatment: Kinetics, mechanisms, and products analysis. *Chem. Eng. J.* **2015**, *271*, 214–222.
- (29) Yang, X.; Flowers, R. C.; Weinberg, H. S.; Singer, P. C. Occurrence and removal of pharmaceuticals and personal care products (PPCPs) in an advanced wastewater reclamation plant. *Water Res.* **2011**, *45*, 5218–5228.
- (30) Dodd, M. C.; Huang, C.-H. Transformation of the Antibacterial Agent Sulfamethoxazole in Reactions with Chlorine: Kinetics, Mechanisms, and Pathways. *Environ. Sci. Technol.* **2004**, *38*, 5607–5615.
- (31) Karaolia, P.; Michael, I.; García-Fernández, I.; Agüera, A.; Malato, S.; Fernández-Ibáñez, P.; Fatta-Kassinos, D. Reduction of clarithromycin and sulfamethoxazole-resistant *Enterococcus* by pilot-scale solar-driven Fenton oxidation. *Sci. Total Environ.* **2014**, *468*–469, 19–27.
- (32) Miao, X.-S.; Bishay, F.; Chen, M.; Metcalfe, C. D. Occurrence of Antimicrobials in the Final Effluents of Wastewater Treatment Plants in Canada. *Environ. Sci. Technol.* **2004**, *38*, 3533–3541.
- (33) Mawhinney, D. B.; Vanderford, B. J.; Snyder, S. A. Transformation of 1H-benzotriazole by ozone in aqueous solution. *Environ. Sci. Technol.* **2012**, *46* (13), 7102–7111.
- (34) Yang, B.; Ying, G.-G.; Zhang, L.-J.; Zhou, L.-J.; Liu, S.; Fang, Y.-X. Kinetics modeling and reaction mechanism of ferrate(VI) oxidation of benzotriazoles. *Water Res.* **2011**, *45*, 2261–2269.
- (35) Zhang, S.; Gitungo, S.; Dyksen, J. E.; Raczko, R. F.; Axe, L. Indicator Compounds Representative of Contaminants of Emerging Concern (CECs) Found in the Water Cycle in the United States. *Int. J. Environ. Res. Public Health* **2021**, *18* (3), 1288.
- (36) Snyder, S. A.; Westerhoff, P.; Yoon, Y.; Sedlak, D. L. Pharmaceuticals, personal care products, and endocrine disruptors in water: Implications for the water industry. *Environ. Eng. Sci.* **2003**, *20* (5), 449–469.
- (37) Xu, B. B.; Wu, F. C.; Zhao, X. L.; Liao, H. Q. Benzotriazole removal from water by Zn-Al-O binary metal oxide adsorbent: Behavior, kinetics and mechanism. *J. Hazard. Mater.* **2010**, *184* (1–3), 147–155.
- (38) Hart, D. S.; Davis, L. C.; Erickson, L. E.; Callender, T. M. Sorption and partitioning parameters of benzotriazole compounds. *Microchem. J.* **2004**, *77* (1), 9–17.
- (39) Chowdhury, I. R.; Chowdhury, S.; Mazumder, M. A. J.; Al-Ahmed, A. Removal of lead ions (Pb(2+)) from water and wastewater: a review on the low-cost adsorbents. *Appl. Water Sci.* **2022**, *12* (8), 185.
- (40) Pinter, J.; Jones, B. S.; Vriens, B. Loads and elimination of trace elements in wastewater in the Great Lakes basin. *Water Res.* **2022**, *209*, No. 117949.
- (41) Lee, Y.; Kovalova, L.; McArdell, C. S.; von Gunten, U. Prediction of micropollutant elimination during ozonation of a hospital wastewater effluent. *Water Res.* **2014**, *64*, 134–148.
- (42) Lee, Y.; Yoon, J.; Von Gunten, U. Spectrophotometric determination of ferrate (Fe(VI)) in water by ABTS. *Water Res.* **2005**, *39* (10), 1946–1953.
- (43) Burton, F. L.; Tchobanoglous, G.; Tsuchihashi, R.; Stensel, H. D.; Metcalf; Eddy, I. *Wastewater Engineering: Treatment and Resource Recovery*; McGraw-Hill Education: New York, NY, USA 2013.
- (44) Steigerwald, J. M.; Peng, S.; Ray, J. R. Novel Perfluorooctanesulfonate-Imprinted Polymer Immobilized on Spent Coffee Grounds Biochar for Selective Removal of Perfluoroalkyl Acids in Synthetic Wastewater. *ACS ES&T Eng.* **2023**, *2*, 100025.
- (45) Ling, Y.; Alzate-Sanchez, D. M.; Klemes, M. J.; Dichtel, W. R.; Helbling, D. E. Evaluating the effects of water matrix constituents on micropollutant removal by activated carbon and β -cyclodextrin polymer adsorbents. *Water Res.* **2020**, *173*, No. 115551.
- (46) Rodríguez-Chueca, J.; Polo-López, M. I.; Mosteo, R.; Ormad, M. P.; Fernández-Ibáñez, P. Disinfection of real and simulated urban wastewater effluents using a mild solar photo-Fenton. *Appl. Catal., B* **2014**, *150*, 619–629.
- (47) Manger, G. E. A Mineral Analysis of Some Common Sands and Their Silica Content. *J. Sediment. Res.* **1934**, *4* (3), 141–151.
- (48) Dong, S.; Mu, Y.; Sun, X. Removal of toxic metals using ferrate(VI): a review. *Water Sci. Technol.* **2019**, *80* (7), 1213–1225.
- (49) Masue, Y.; Loeppert, R. H.; Kramer, T. A. Arsenate and arsenite adsorption and desorption behavior on coprecipitated aluminum:iron hydroxides. *Environ. Sci. Technol.* **2007**, *41* (3), 837–842.
- (50) Rush, J. D.; Zhao, Z.; Bielski, B. H. J. Reaction of Ferrate(VI)/Ferrate(V) with Hydrogen Peroxide and Superoxide Anion - a Stopped-Flow and Premix Pulse Radiolysis Study. *Free Radical Res.* **1996**, *24* (3), 187–198.
- (51) Yu, J.; Jiao, R.; Sun, H.; Xu, H.; He, Y.; Wang, D. Removal of microorganic pollutants in aquatic environment: The utilization of Fe(VI). *J. Environ. Manage.* **2022**, *316*, No. 115328.
- (52) Kamachi, T.; Kouno, T.; Yoshizawa, K. Participation of multioxidants in the pH dependence of the reactivity of ferrate(VI). *J. Org. Chem.* **2005**, *70* (11), 4380–4388.
- (53) Zhang, Y. T.; Liu, C.; Xu, B. B.; Qi, F.; Chu, W. Degradation of benzotriazole by a novel Fenton-like reaction with mesoporous Cu/MnO: Combination of adsorption and catalysis oxidation. *Appl. Catal., B* **2016**, *199*, 447–457.
- (54) Miao, Y. X.; Wang, S. L.; Wang, C. W.; Liu, Y. L.; Sun, M. B.; Chen, Y. Effect of chelating agent on benzotriazole removal during post copper chemical mechanical polishing cleaning. *Microelectron. Eng.* **2014**, *130*, 18–23.
- (55) Finsgar, M.; Milosev, I. Inhibition of copper corrosion by 1,2,3-benzotriazole: A review. *Corros. Sci.* **2010**, *52* (9), 2737–2749.
- (56) Kim, H. C.; Kim, M. J.; Lim, T.; Park, K. J.; Kim, K. H.; Choe, S.; Kim, S. K.; Kim, J. J. Effects of nitrogen atoms of benzotriazole and its derivatives on the properties of electrodeposited Cu films. *Thin Solid Films* **2014**, *550*, 421–427.
- (57) Costarramone, N.; Kneip, A.; Castetbon, A. Ferrate(VI) oxidation of cyanide in water. *Environ. Technol.* **2004**, *25* (8), 945–955.
- (58) Yngard, R.; Damrongsiri, S.; Osathaphan, K.; Sharma, V. K. Ferrate(VI) oxidation of zinc-cyanide complex. *Chemosphere* **2007**, *69* (5), 729–735.
- (59) Tiwari, D.; Sailo, L.; Pachau, L. Remediation of aquatic environment contaminated with the iminodiacetic acid metal complexes using ferrate(VI). *Sep. Purif. Technol.* **2014**, *132*, 77–83.
- (60) Wang, S.; Shao, B.; Qiao, J.; Guan, X. Application of Fe(VI) in abating contaminants in water: State of art and knowledge gaps. *Front. Environ. Sci. Eng.* **2021**, *15* (5), 80.
- (61) Sharma, V. K.; Zboril, R.; Varma, R. S. Ferrates: greener oxidants with multimodal action in water treatment technologies. *Acc. Chem. Res.* **2015**, *48* (2), 182–191.
- (62) Qutob, M.; Hussein, M. A.; Alamry, K. A.; Rafatullah, M. A review on the degradation of acetaminophen by advanced oxidation process: pathway, by-products, biotoxicity, and density functional theory calculation. *RSC Adv.* **2022**, *12* (29), 18373–18396.
- (63) Li, C.; Li, X. Z.; Graham, N. A study of the preparation and reactivity of potassium ferrate. *Chemosphere* **2005**, *61* (4), 537–543.
- (64) Jebalbarezi, B.; Dehghanzadeh, R.; Sheikhi, S.; Shahmahdi, N.; Aslani, H.; Maryamabadi, A. Oxidative degradation of sulfamethoxazole from secondary treated effluent by ferrate(VI): kinetics, by-products, degradation pathway and toxicity assessment. *J. Environ. Health Sci. Eng.* **2022**, *20*, 205–218.

(65) Sharma, V. K.; Mishra, S. K.; Nesnas, N. Oxidation of Sulfonamide Antimicrobials by Ferrate(VI) $[\text{Fe}^{\text{VI}}\text{O}_4^{2-}]$. *Environ. Sci. Technol.* **2006**, *40* (23), 7222–7227.

(66) Jahdi, M.; Mishra, S. B.; Nxumalo, E. N.; Mhlanga, S. D.; Mishra, A. K. Smart pathways for the photocatalytic degradation of sulfamethoxazole drug using F-Pd co-doped TiO₂ nanocomposites. *Appl. Catal., B* **2020**, *267*, No. 118716.

(67) Wang, H. Y.; Liu, Y. B.; Jiang, J. Q. Reaction kinetics and oxidation product formation in the degradation of acetaminophen by ferrate (VI). *Chemosphere* **2016**, *155*, 583–590.

(68) Manoli, K.; Nakhla, G.; Ray, A. K.; Sharma, V. K. Oxidation of caffeine by acid-activated ferrate(VI): Effect of ions and natural organic matter. *AIChE J.* **2017**, *63* (11), 4998–5006.

(69) Feng, M.; Wang, X.; Chen, J.; Qu, R.; Sui, Y.; Cizmas, L.; Wang, Z.; Sharma, V. K. Degradation of fluoroquinolone antibiotics by ferrate(VI): Effects of water constituents and oxidized products. *Water Res.* **2016**, *103*, 48–57.

(70) Ma, L.; Lam, W. W. Y.; Lo, P. K.; Lau, K. C.; Lau, T. C. Ca-Induced Oxygen Generation by FeO at pH 9–10. *Angew. Chem. Int. Ed.* **2016**, *55* (9), 3012–3016.

(71) Sarma, R.; Angeles-Boza, A. M.; Brinkley, D. W.; Roth, J. P. Studies of the Di-iron(VI) Intermediate in Ferrate-Dependent Oxygen Evolution from Water. *J. Am. Chem. Soc.* **2012**, *134* (37), 15371–15386.